REDUCTION OF HELICOPTER BVI NOISE, VIBRATION, AND POWER CONSUMPTION THROUGH INDIVIDUAL BLADE CONTROL

Stephen A. Jacklin
NASA Ames Research Center
Moffett Field, California

Achim Blaas
ZF Luftfahrttechnik, GmbH
Kassel-Calden, Germany

Dietrich Teves
Eurocopter Deutschland, GmbH
Munchen, Germany

Roland Kube
DLR Institute for Flight Mechanics
Braunschweig, Germany

Abstract

A full-scale wind tunnel test was conducted to evaluate the potential of helicopter individual blade control (IBC) to improve rotor performance, to reduce blade vortex interaction (BVI) noise, and to alleviate helicopter vibrations. The pitch links of the rotor were replaced by servo-actuators to enable the pitch of each blade to be controlled independently of the other blades. The IBC servo-actuators and control system were designed and manufactured by ZF Luftfahrttechnik, GmbH. This wind tunnel test of a full-scale IBC system was the second of two conducted in the 40- by 80-Foot Wind Tunnel at the NASA Ames Research Center using a BO 105 helicopter rotor. The acquired data set includes data on rotor performance, the static and dynamic hub forces and moments, rotor loads, control system loads, inboard and outboard blade pitch motion, and BVI noise. The data indicated that very significant (85 percent) simultaneous reductions in both BVI noise and hub vibrations could be obtained using multi-harmonic IBC input. The data also showed that performance improvements of up to 7 percent could be obtained using 2/rev input at high-speed forward flight conditions.

The IBC test program was an international collaborative effort between NASA, the U.S. Army AFDD, ZF Luftfahrttechnik, Eurocopter Deutschland, and the DLR Institute of Flight Mechanics and was conducted under the auspices of the U.S./German Memorandum of Understanding on Helicopter Aeromechanics.

Presented at the American Helicopter Society 51st Annual Forum, Fort Worth, TX, May 9-11, 1995.

Notation

BVI	blade vortex interaction
C_T/σ	rotor thrust coefficient
D_{EQ}	equivalent airframe drag area, ft^2
IBC	individual blade control
N	number of blades
n	IBC input harmonic number
n/rev	"n" cycles per rotor revolution
Q	rotor shaft torque, ft-lbs
RTA	NASA/U.S. Army Rotor Test Apparatus
q	dynamic pressure
R	rotor radius, 16.1 ft
Ω	revolution speed, 44.4 rad/sec
Ψ	rotor azimuth angle, deg
α_S	shaft angle, deg
μ	advance ratio
θ_i	pitch of ith blade
σ	rotor solidity, 0.07

Introduction

Helicopter control through the conventional swashplate is fundamentally limited for rotor systems having four or more main rotor blades. The three degrees of freedom afforded by the conventional swashplate (1 collective and 2 cyclic) allow the individual pitch control of up to three blades at most. Whereas this shortcoming of the conventional swashplate poses no problems for maintaining helicopter trim in forward flight, it does limit the degrees of freedom available for improving rotor performance, reducing rotorcraft vibrations, and reducing helicopter noise.

Although individual blade control (IBC) has long been proposed as a method for reducing helicopter vibrations and improving helicopter performance [Refs. 1-6], most of the work in this area has centered on active control schemes using actuators in the fixed system. The most prevalent of these methods, the higher harmonic control (HHC) method, was thoroughly tested through analysis, wind tunnel, and flight testing. These investigations have shown that HHC can be used very effectively to reduce helicopter vibrations [Refs. 7-14]. More recently it has been shown that HHC can also be used to achieve moderate reductions in helicopter blade-vortex interactional (BVI) noise [Refs. 15-17]. However, the HHC inputs needed to produce the best BVI noise reductions have been found to be different from those needed for good vibration reduction.

Individual blade control may offer a solution for this problem. By having more degrees of freedom, simultaneous control of both noise and vibration may be achieved. Although not as straight-forward to implement as HHC, some of the conceptual designs proposed to implement IBC also offer the possibility of reducing the weight of the active control system [Ref. 18]. The difficulty, of course, is that for rotors having four (or more) blades, attainment of individual blade control is possible only through the placement of actuators in the rotating system, one per blade.

Desiring to pursue the dream of individual blade control, ZF Luftfahrttechnik, GmbH, began the development of IBC actuators more than a decade ago. Designed to replace the pitch links of the rotor system, these actuators were initially proposed for automatic, in-flight rotor blade tracking adjustment. Nevertheless, this use of actuators in the rotating system, one for each blade, represented a breakthrough in rotor control technology. During the 1980s, the reliability of the control system was improved and the bandwidth of the actuators was increased to produce controls in the frequency range needed for active helicopter vibration reduction.

In 1990 and 1991, ZF Luftfahrttechnik and Eurocopter Deutchland (ECD) conducted the first flight tests of a prototype IBC system on a BO 105 helicopter. The flight tests indicated that vibration reduction was possible using IBC [Refs. 19 and 20]. However, because the stroke of the actuators was restricted (for safety reasons) to 0.25 deg in 1990 and to 0.49 deg in 1991, a full exploration of the IBC system capability was not possible. In addition, the limited speed of the aircraft precluded the testing of 2/rev IBC to increase rotor performance at high-speed conditions.

In order to explore the full potential of individual blade control, a full-scale wind tunnel test program was proposed using the NASA Ames 40- x 80-Foot Wind Tunnel and a new IBC system having greater control authority and increased frequency response. The testing was part of an international collaborative effort between NASA, the U.S. Army AFDD, ZF Luftfahrttechnik GmbH, Eurocopter Deutschland GmbH, and the DLR Institute for Flight Mechanics and was conducted under the auspices of the U.S./German MOU on Helicopter Aeromechanics. In addition to testing IBC for its ability to reduce vibration and improve rotor performance, NASA proposed testing the IBC system for its ability to reduce blade vortex interaction (BVI) noise as well. The interested reader is referred to Ref. 21 for a full discussion of the plans and preparations made to support the first wind tunnel test effort, and to Ref. 22 for a complete description of the IBC hardware and control system.

In 1993, the first of two IBC wind tunnel tests was conducted at the NASA Ames 40- by 80-Foot Wind Tunnel. Single-frequency, multi-frequency, wavelet, and pulse type IBC inputs were studied. This test clearly indicated that IBC could be used to suppress all vibratory hub shears and moments by up to 70 percent at the transition speed $\mu = 0.1$ [Ref. 23]. A 7 db reduction in BVI noise was also observed at a descent flight condition showing high BVI noise levels ($\mu = 0.15$) [Ref. 24]. These results were very encouraging. However, the test program could not evaluate the capability of IBC to improve rotor performance at high-speed because of a limitation in the Ames Rotor Test Apparatus (RTA) primary control system. A second shortcoming was that the use multi-harmonic IBC inputs to achieve simultaneous noise and vibration reduction were not evaluated at the same test condition.

To achieve these objectives, a second IBC test was conducted in 1994 after the RTA primary control system had been strengthened. The increase in load carrying capability, however, was not beyond the strength limits of the standard BO 105 helicopter pitch horn, blades, and hub flight hardware. Open-loop IBC input was evaluated at flight conditions ranging from low-speed descent to forward flight at speeds of up to 190 kts ($\mu = 0.45$). The IBC inputs consisted of single-frequency inputs from 2/rev to 6/rev and various multi-harmonic combinations at amplitudes up to 2.5 deg, where "2/rev IBC" denotes a sinusoidal blade pitch input at a frequency of 2 cycles per rotor revolution.

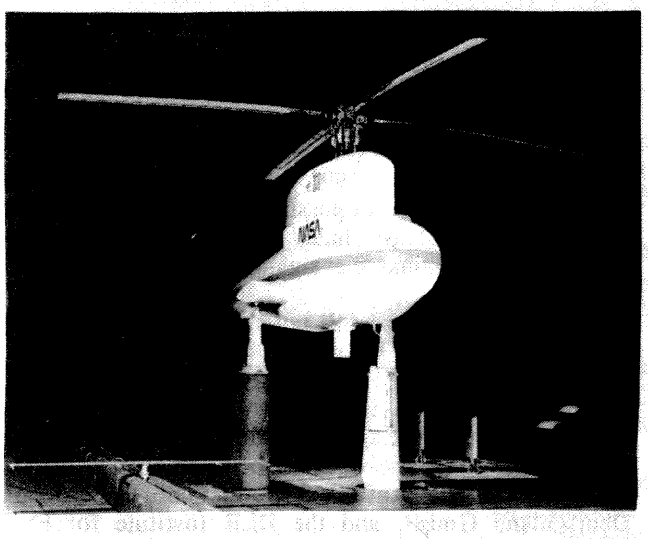

Figure 1. Installation of the RTA and BO 105 rotor in the NASA Ames 40- by 80-Foot Wind Tunnel.

Test Hardware and Instrumentation

The IBC tests were performed in the NASA Ames 40- by 80-Foot Wind Tunnel. The test section of this closed-circuit wind tunnel is treated with sound absorptive material to allow near-anechoic acoustic measurements down to 500 Hz. Airspeeds of up to 300 kts may be achieved.

For the IBC testing, a four-bladed, hingeless, BO 105 rotor was mounted to the NASA/U.S. Army Rotor Test Apparatus (Fig. 1). This rotor had a radius of 16.1 ft, a linear blade twist of 8 deg, a solidity of 0.07, and NACA 23012 airfoils. The rotor blades, pitch horns, and hub were standard BO 105 helicopter flight hardware owned by NASA.

The IBC actuators replaced the normal BO 105 rotor system pitch links, as shown in Fig. 2. References 21-23 provide a full discussion of the IBC servo-mechanism arrangement, the IBC actuator characteristics, the automatic emergency shutdown features used to maintain system safety, and the computer system used to control the IBC actuators. These

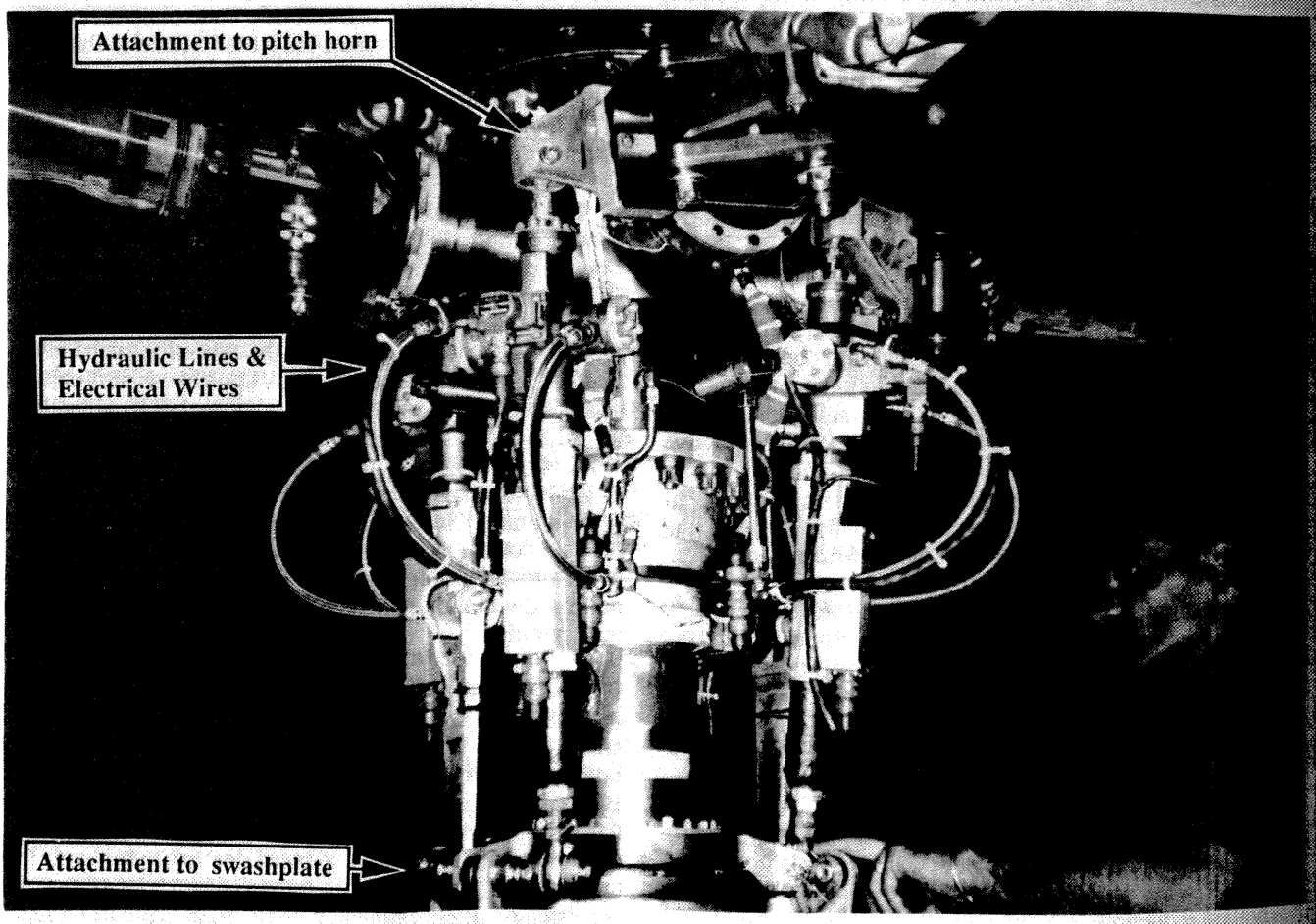

Figure 2. Rotor hub showing placement of IBC actuators.

references also explain in detail how the RTA was modified for the IBC test to permit the transfer of hydraulic fluid to the IBC actuators in the rotating system.

Table 1 presents a list of the instrumentation placed on the rotor blades, control system, and test stand. Strain gages were used to measure loads on the blades and control system. The IBC motion at the blade tip was calculated from miniature accelerometers located at the blade tip and oriented to measure rotation (Ref. 23). Miniature surface-mounted pressure transducers were used to detect the presence of blade-vortex interactions at four leading edge blade locations.

The RTA static/dynamic rotor balance was used to measure the rotor thrust, side force, drag force, pitching moment and rolling moment. These forces and moments were transformed into forces and moments in the hub plane. Both averaged and time-history loads were measured. The time history data provided information on the vibratory hub loads.

The rotor shaft was instrumented with two sets of strain gages. The first set was used to measure the shaft torque, from which the total power needed to turn the rotor, $(\Omega \cdot R) \cdot Q$, could be calculated. This total power was equal to the sum of the induced, profile, and propulsive power generated in the wind tunnel. The second set of strain gages measured the shaft bending moments.

The displacements and forces of both the stationary swashplate control actuators and the rotating IBC actuators were measured. Each IBC actuator had two LVDTs to provide a dual position measurement. Loads on the control system were evaluated by measuring the axial forces (or pitch link loads) developed in each of the four IBC actuators and each of the three control rods which controlled the swashplate attitude in the fixed-system. In addition, the root pitch of each blade was measured using resistive strips at the pitch bearing.

Acoustic data were gathered using a four-microphone traverse system located below the advancing side of the rotor and three fixed microphones located below and aft on the retreating side (Fig. 3 and Table 2). The advancing side microphones were fixed in the lateral and vertical directions and moved by the traverse in the stream-wise direction. Because data acquisition with the traverse was time-consuming, only a single position of the traverse was used for most data points. To document the directivity effects for

Table 1. Instrumentation.

Measurement	Location and Number
Rotor Blade:	Location, in (R=193.2 in)
Blade Flap Bending	20, 110 in
Blade Chord Bending	28, 110 in
Blade Torsion Moment	65, 77, 110, 155 in
Blade Pressures	116, 135, 155, 174 in
Blade Accelerometers	58, 97, 135 in (flapwise)
Blade Tip Accelerometers	Leading & Trailing Edges
Rotor Balance:	Lift, Side, and Drag Forces Pitch and Roll Moments
Rotor Mast:	
Flex-coupling	Shaft Torque
Rotor Shaft	Shaft Bending Moment
Control System:	
IBC Actuator Position	8 (2 per Actuator)
IBC Actuator Forces	4 (1 per Actuator)
Swashplate Position	3 (1 per Control Rod)
Swashplate Link Force	3
Rotating Scissors	2
Stationary Scissors	1
Blade Pitch Transducers	4 (1 per blade)
Microphones:	
Stationary	3, retreating side
Traverse	4, advancing side

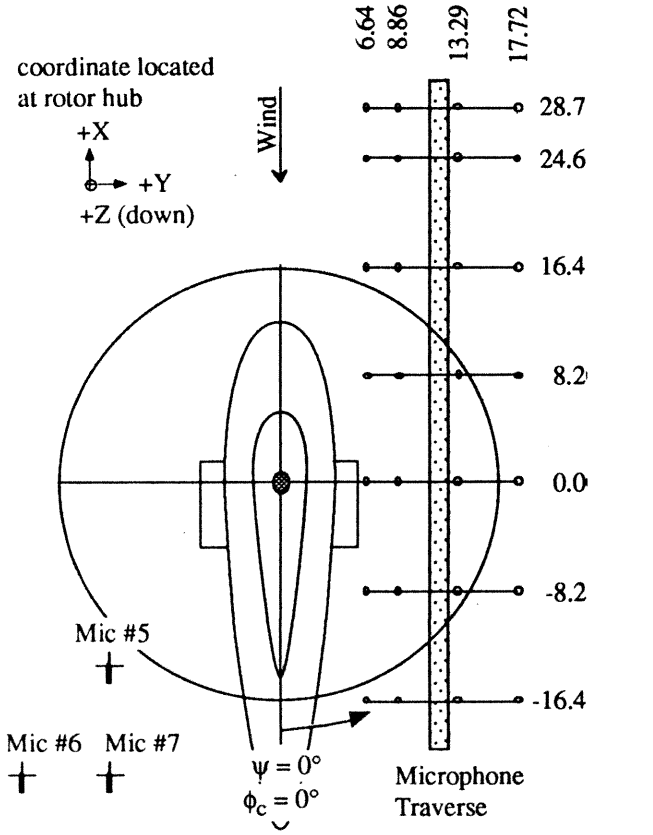

Figure 3. General layout of the microphones relative to the rotor hub center and RTA; all dimensions in feet.

Table 2:
Microphone Positions Relative to the Rotor Hub Center, ft.

	X	Y	Z
Mic 1	*	17.72	18.86
Mic 2	*	13.29	18.86
Mic 3	*	8.86	18.86
Mic 4	*	6.64	18.86
Mic 5	-6.62	-13.29	14.12
Mic 6	-14.62	-13.29	14.12
Mic 7	-14.62	-8.86	14.12

* Variable. See Fig. 3 for the 7 locations.

IBC inputs producing substantial BVI noise reductions, the traverse was moved streamwise to acquire data at 6 other positions on the advancing side of the rotor.

Definition of IBC Inputs

The IBC pitch input is defined

$$\theta_i = A \cdot Cos\left[n\left(\Psi_1 - (i-1)(90\text{deg})\right) - \phi \right] \qquad (1)$$

where θ_i is the pitch of the ith rotor blade, A is the amplitude, n is the IBC harmonic, Ψ_1 is the rotor azimuth angle of blade No. 1 (measured from 0 deg aft), and ϕ is the phase angle of the IBC input. This equation defines the same pitch schedule for each blade relative to its physical azimuth location in the rotor plane. All blades have the same pitch schedule around the azimuth.

To help understand the physics, it is sometimes useful to know the spatial orientation of the IBC input blade pitch. In this paper, ϕ is termed the IBC input phase angle and is used extensively in all of the plots presented herein. It is important to recognize that this phase angle refers to the phase of the control input, not to the rotor azimuth angle, Ψ. For any single-frequency IBC input, the azimuth location of the first maximum blade pitch peak is at rotor azimuth angle of (ϕ/n) deg. The other "n" peaks are located at multiples of (360/n) rotor azimuth angle degs from the first peak. For example, in Fig. 4 the blade pitch added by a 1.0 deg amplitude, 2/rev IBC input at an IBC phase angle of 270 deg is shown. The first peak of this 2/rev "cosine" input has been shifted (270/2) rotor azimuth angle degrees to the right. A second peak follows (360/2) rotor azimuth angle degrees later. Table 3 indicates the location of the first maximum pitch angle as a function of n and ϕ. Obviously, the minima are located halfway between adjacent peaks.

Two caveats must be remembered when determining the pitch displacement history. First, as explained in Ref. 23, the blade torsional dynamics make the IBC input magnitudes and phases at the blade tip different from those introduced at the blade root. Using the accelerometer data obtained from the blade tip, the approximate phase shifts for each harmonic at the blade tip were calculated and are presented in the last column of Table 3. Second, the 1/rev cyclic trim inputs used to maintain constant hub moment trim were always added to the n/rev IBC inputs. The 1/rev inputs had a considerable effect on the total blade pitch angle, especially for 2/rev and 3/rev IBC inputs. The best understanding of the blade pitch history is gained from the measured blade root pitch angle. The pitch angle at the blade tip can then be found by adjusting the gain and shifting the phase of the IBC input harmonics using the values provided in Ref. 23.

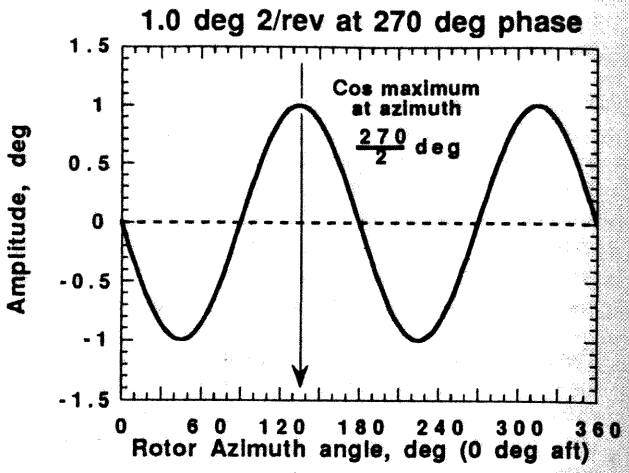

Figure 4: 1.0 deg of 2/rev IBC input at an input phase angle of 270 deg.

Table 3.
Azimuth location of IBC peak pitch inputs.*

Harmonic (no. peaks)	Spacing Between Peaks	Location of First Peak (Blade Root)	Location of First Peak (Blade Tip)
2/rev	180 deg	ϕ/2 deg	ϕ/2 + 10 deg
3/rev	120 deg	ϕ/3 deg	ϕ/3 + 13 deg
4/rev	90 deg	ϕ/4 deg	ϕ/4 + 33 deg
5/rev	72 deg	ϕ/5 deg	ϕ/5 + 42 deg
6/rev	60 deg	ϕ/6 deg	ϕ/6 + 34 deg

* All locations in degrees of rotor azimuth angle, Ψ.

Test Results

Most of the wind tunnel testing was performed at the nominal rotor speed of 425 RPM and the rotor thrust trimmed to 1g ($C_T/\sigma = 0.075$). The IBC data were acquired primarily at the six conditions shown in Table 4. These

Table 4. IBC Trim Conditions.

Cond. No.	Adv. Ratio, μ (Speed)	Thrust Coeff. C_T/σ	Shaft Angle α_s	Hub Pitch Moment	Hub Roll Moment	Propulsive Force	Equiv. Des. Velocity
1	.1 (43 kts)	0.075	-2.4 deg	1,400 ft-lb	-300 ft-lb	210 lbs	-----
2	.1 (43 kts)	0.075	4.0 deg	1,400 ft-lb	-300 ft-lb	-----	446 ft/min*
3	.15 (65 kts)	0.075	2.9 deg	1,600 ft-lb	-350 ft-lb	-----	630 ft/min**
4	.3 (127 kts)	0.075	-7.6 deg	1,600 ft-lb	-950 ft-lb	670 lbs	-----
5	.4 (169 kts)	0.075	-9.0 deg	1,000 ft-lb	-1,750 ft-lb	780 lbs	-----
6	.45 (190 kts)	0.070	-8 deg	1,000 ft-lb	-1,750 ft-lb	640 lbs	-----

* Equivalent to 5.87 deg glide slope. ** Equivalent to 5.55 deg glide slope.

conditions were: 1) a low-speed forward-flight condition producing high vibration, 2) a descent flight condition having both moderately high BVI noise and vibration, 3) a descent flight condition showing the highest BVI noise, and 4-6) high-speed forward flight conditions for performance improvement studies using 2/rev IBC. A limited amount of vibration control work was also done at condition 4 (127 kts).

In addition to maintaining thrust trim, the 1/rev cyclic control input from the swashplate was adjusted to maintain constant pitch and roll moments for each flight condition. These trim hub moments were estimated from flight test data and are listed in Table 4. Because the hub moments indicated the attitude of the tip-path plane with respect to the shaft, they directly influenced the orientation of the thrust vector with respect to the free stream velocity. Constant moment and thrust trim combined with a fixed shaft angle therefore lead to a constant propulsive force and lift which was needed in order to simulate the rotor in forward flight in the wind tunnel. Therefore, the hub moments and thrust were re-trimmed with each new IBC input in order make sure that the rotor was operating at the same conditions with and without IBC excitation.

Some of the key test results showing the effect of IBC on vibration, BVI noise, and power consumption are presented below.

IBC for Vibration Control

Since the RTA was not structurally or dynamically representative of an actual helicopter fuselage, the best characterization of the vibration was obtained through examination of the vibratory forces and moments produced at the rotor hub. These were measured by the RTA rotor balance and then transformed into forces and moments in the hub plane system. Frequency analysis of the hub lift force, side force, drag force, rolling moment, and pitching moment showed that most of the vibratory energy was contained in the fourth harmonic. This, of course, was expected for a 4-bladed rotor since only multiples of the N/rev vibration tend to be transmitted to the fixed system [Ref. 25]. Therefore, in the following discussion, the capability of IBC to alleviate helicopter vibration is explained in the context of controlling the 4/rev vibration component.

The ability of IBC to suppress the vibratory hub loads was tested primarily at condition 1 listed in Table 4 (43 kts, -2.4 deg shaft angle). This condition represented the high vibration found during transition between hover and forward flight. In addition, some testing was also done at condition 4 to evaluate the effects of IBC on vibration at cruise speed.

The IBC inputs were introduced one harmonic at a time. The amplitude was fixed while the phase of the input was varied. Data was collected at several IBC input phase angles. At the phase angle producing the best vibration reduction (if any), the IBC amplitude was varied.

Although time history data was collected for all of the rotor hub forces and moments, it is expedient to apply the relationships

$$Shear = \sqrt{(Side\ Force)^2 + (Drag\ Force)^2}$$
$$Moment = \sqrt{(Pitch\ Moment)^2 + (Roll\ Moment)^2} \quad (2)$$

to the 4/rev hub forces and moments. This reduces the vibratory degrees of freedom and allows better expression of the total vibration reduction achieved. If the moments and forces were not combined, vibratory energy in the pitching moment or side force could be transferred to the rolling moment or drag force with no net vibration reduction.

Low-Speed Vibration. The following plots show the effect of IBC on the low-speed vibrations found at the transition speed (43 kts). The vertical axis has units of percent change in the baseline 4/rev vibration. By plotting the percent change, presentation of the baseline forces and moments is not required.

Figure 5 presents the effect of 1.0 deg of 2/rev IBC on the hub vibration. It is seen that the 4/rev forces and moments were best reduced using an input phase angle of about 60 deg. Variation of the input amplitude at this phase, showed that the 4/rev hub shears and moments could be simultaneously reduced by 70-80 percent using 2.5 deg of 2/rev IBC input (Fig. 6). About half the baseline 4/rev lift force (vertical shear force) could be eliminated at the same time. However, where as the shear and moment decreased in proportion to the IBC amplitude up to 2.5 deg, most of the reduction in the vertical shear force was obtained with only 1.5 deg of IBC input.

A phase sweep of 1.0 deg of 3/rev IBC, however, showed that the 4/rev vertical shear forces could be almost entirely eliminated using an input phase angle of 150 deg (Fig. 7). Although the 4/rev shear forces and moments were also reduced by 40 percent at that phase angle, they were slightly better reduced at a different phase angle (180 deg). In fact, for most of the IBC inputs, the hub moments and horizontal shear forces were effected in a like manner by the IBC inputs, while the vertical shear force behaved somewhat differently. An amplitude sweep at the 150 deg input phase showed that a 1.0 deg input amplitude produced the best vibration reductions using 3/rev IBC (Fig. 8). Although the percent reduction of the 4/rev shears and moments was different than the percent reduction of the 4/rev vertical lift force, the trend was the same.

Figure 9 shows that 0.5 deg of 4/rev IBC reduced the 4/rev hub shears and moments best at an input phase angle of 240 deg, while the 4/rev lift force was better reduced using a 300 deg phase angle. Variation of the amplitude at the 240 deg input phase showed that the 4/rev shear forces and moments could be simultaneously reduced to 60 percent by increasing the amplitude to 1.0 deg, (Fig. 10). Unfortunately, the vertical shear force was increased at this amplitude.

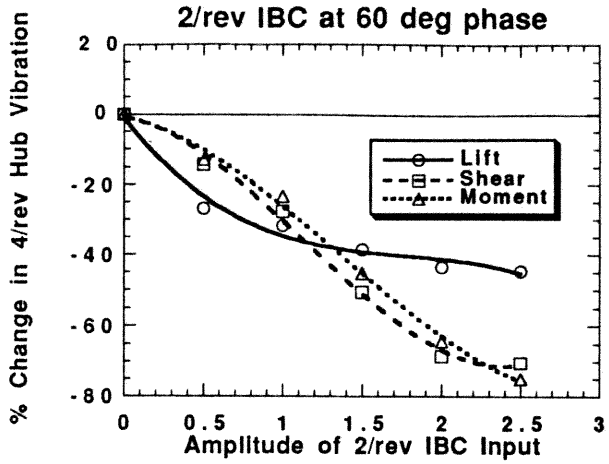

Fig. 6. Amplitude sweep with 2/rev at 60 deg phase for 43 kts, α_S= -2.4 deg, C_T/σ = 0.075.

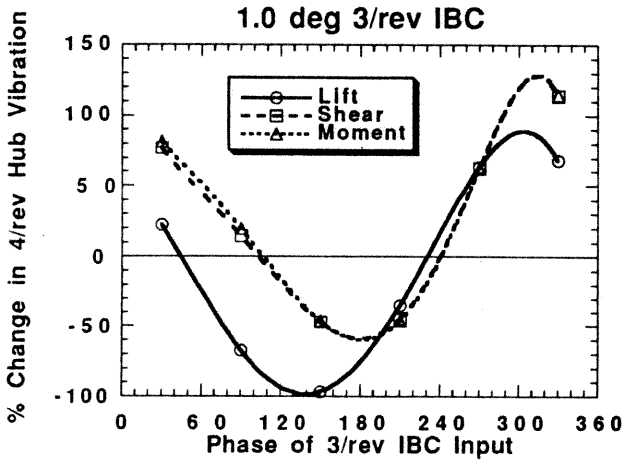

Fig. 7. Phase sweep with 3/rev at 1.0 deg amplitude for 43 kt for α_S= -2.4 deg, C_T/σ = 0.075.

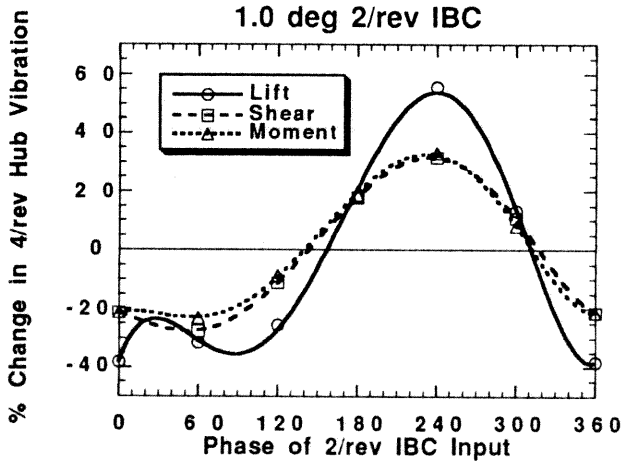

Fig. 5. Phase sweep with 2/rev at 1.0 deg amplitude for 43 kts, α_S= -2.4 deg, C_T/σ = 0.075.

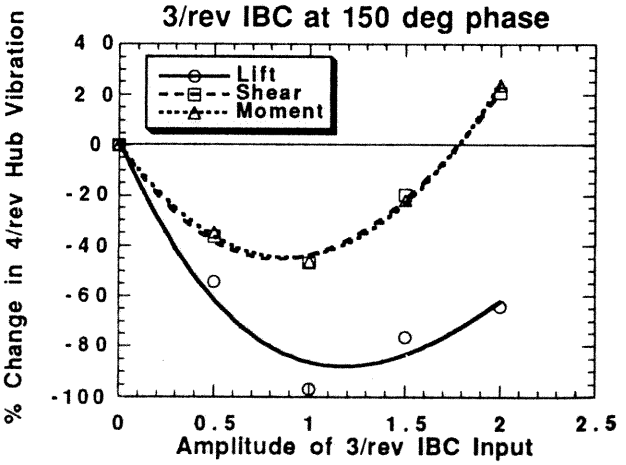

Fig. 8. Amplitude sweep with 3/rev at 150 deg phase for 43 kts, α_S= -2.4 deg, C_T/σ = 0.075.

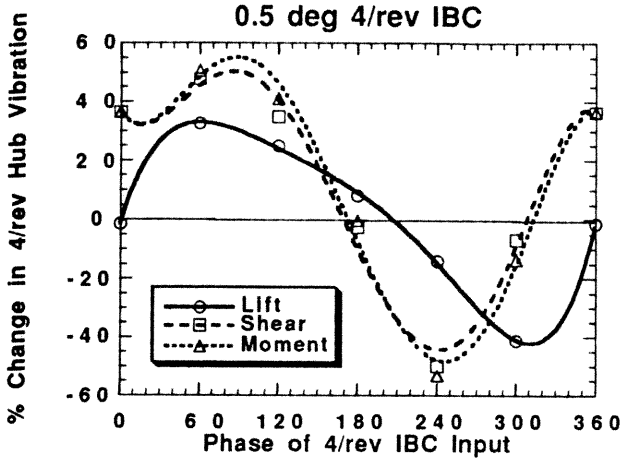

Fig. 9. Phase sweep with 4/rev at 0.5 deg amplitude for 43 kts, α_S= -2.4 deg, C_T/σ = 0.075.

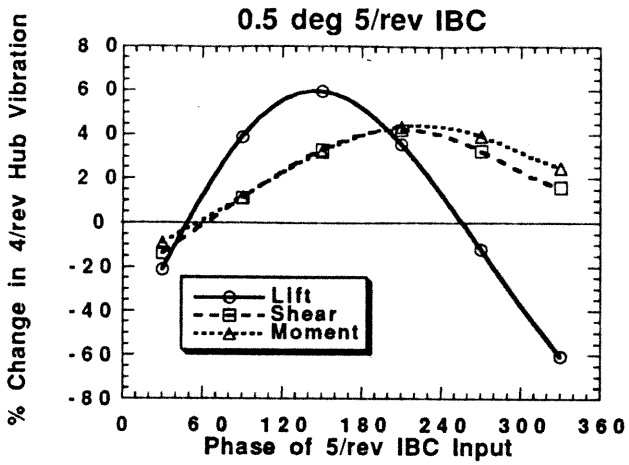

Fig. 11. Phase sweep with 5/rev at 0.5 deg amplitude for 43 kts, α_S= -2.4 deg, C_T/σ = 0.075.

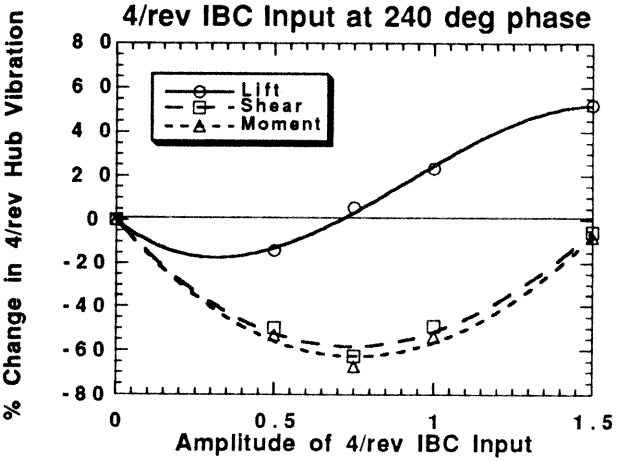

Fig. 10. Amplitude sweep with 4/rev at 240 deg phase for 43 kts, α_S= -2.4 deg, C_T/σ = 0.075.

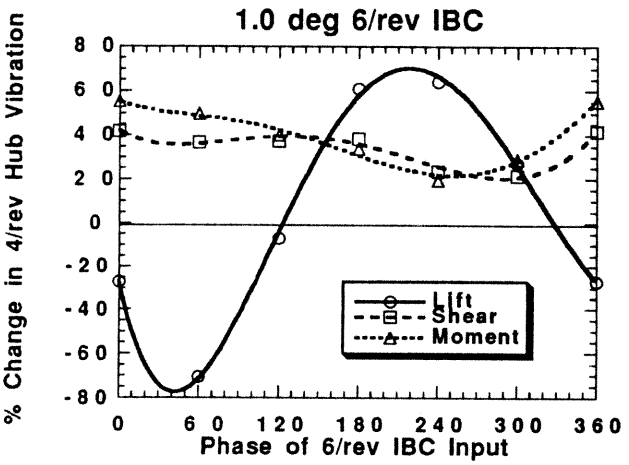

Fig. 12. Phase sweep with 6/rev at 1.0 deg amplitude for 43 kts, α_S= -2.4 deg, C_T/σ = 0.075.

Figures 11 and 12 show that vibration control using 5/rev and 6/rev IBC was usually even less effective than 4/rev IBC. Figure 11 shows that although a 0.5 deg 5/rev IBC input could suppress the 4/rev vertical shear forces by over 60 percent using an input phase angle of 330 deg, the 4/rev hub moment and horizontal shear force were increased about 20 percent at the same time. Similarly, applying 1.0 deg of 6/rev IBC, the vertical shear forces could be suppressed 80 percent with an input phase angle of 45 deg, but the 4/rev hub in-plane shears and moments were increased about 50 percent as well (Fig. 12). Therefore, 5/rev and 6/rev IBC were not considered to be very effective inputs for vibration suppression at low-speed.

Cruise Vibration. Only a brief time was spent examining the effects of 2/rev, 3/rev, and 4/rev IBC on the hub vibrations at 127 kts because the overall vibrations were much less than those found in the transition region. Testing of 2/rev IBC was required for performance evaluation. The 3/rev and 4/rev IBC inputs were tested because of their ability to reduce vibration at low-speed.

Figures 13-15 show the data acquired from application of 2/rev, 3/rev, and 4/rev IBC. As can be seen, these inputs generally produced much higher vibration compared to the baseline condition (no IBC). Since it appeared that none of these harmonics were suitable for vibration reduction, no additional data was acquired at the 127 kt condition.

However, after the test, more information was learned by plotting the 4/rev sine and 4/rev cosine components in a two-dimensional graph, similar to a complex number plane. Figures 16-18 show the effect of 2/rev, 3/rev, and 4/rev IBC on the 4/rev sine vs. cosine of the pitching moment vibration. (Note that 5 plots per rotor balance measurement would be required to represent the full effect.) The baseline cases (without IBC) are represented by dots somewhere off the origin in each of the plots. If the transference between

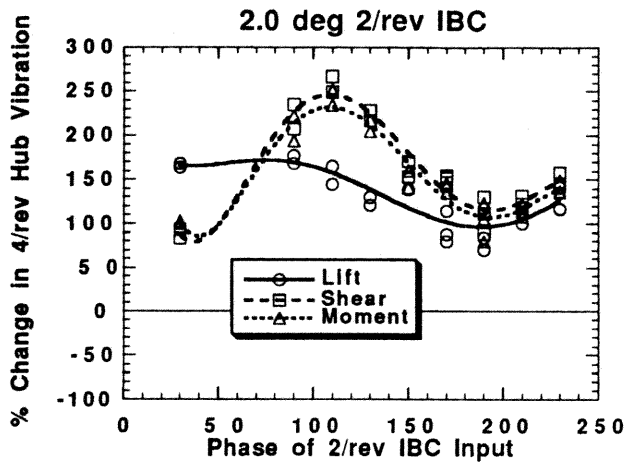

Fig. 13. Phase sweep with 2/rev at 2.0 deg amplitude for 127 kts, α_S= -7.6 deg, C_T/σ = 0.075.

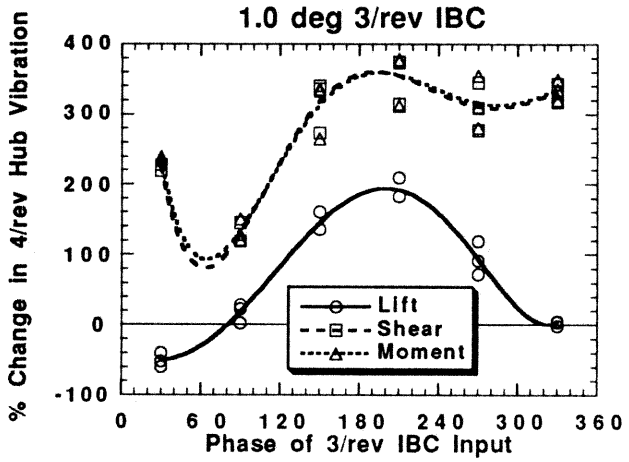

Fig. 14. Phase sweep with 3/rev at 1.0 deg amplitude for 127 kts, α_S= -7.6 deg, C_T/σ = 0.075.

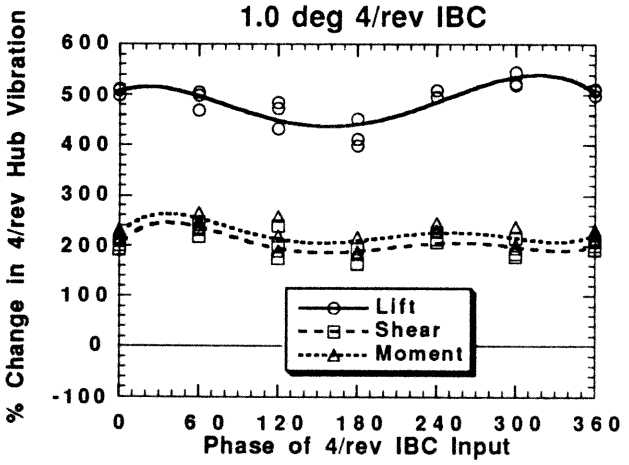

Fig. 15. Phase sweep with 4/rev at 1.0 deg amplitude for 127 kts, α_S= -7.6 deg, C_T/σ = 0.075.

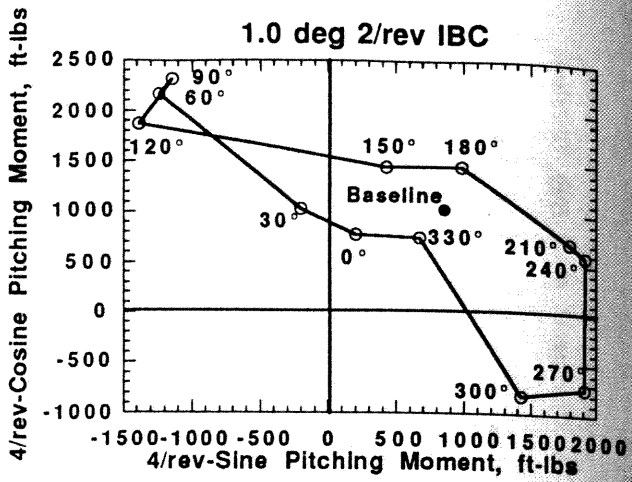

Fig. 16. Phase sweep of 2/rev IBC at 1.0 deg amplitude for 127 kts, α_S = -7.6 deg, C_T/σ = 0.075.

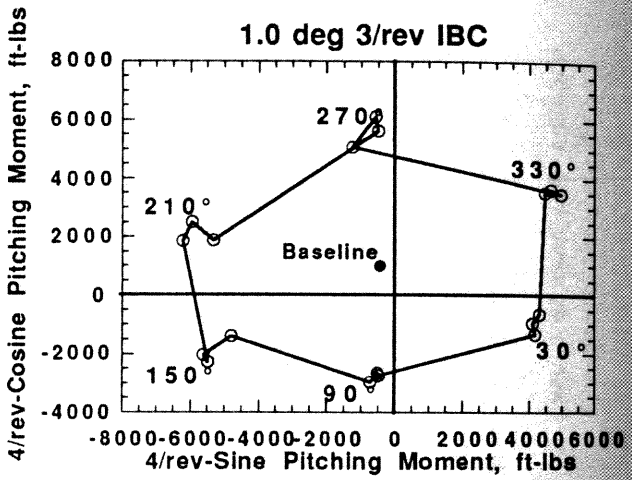

Fig. 17. Phase sweep of 3/rev IBC at 1.0 deg amplitude for 127 kts, α_S= -7.6 deg, C_T/σ = 0.075.

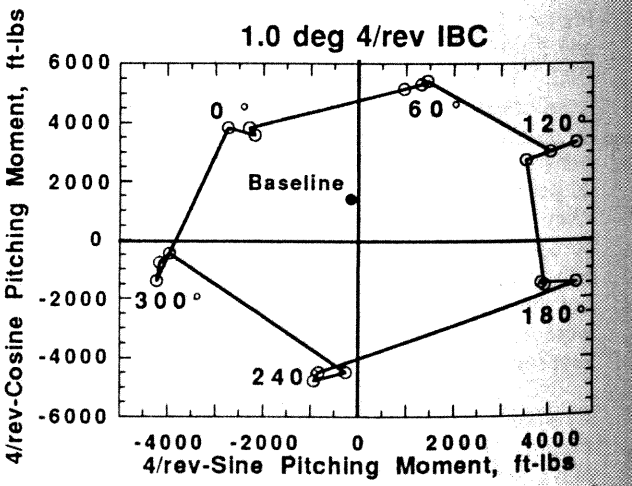

Fig. 18. Phase sweep of 4/rev IBC at 1.0 deg amplitude for 127 kts, α_S= -7.6 deg, C_T/σ = 0.075.

the IBC inputs and 4/rev pitching moment outputs were perfectly linear, then the vibration data would form circles around the baseline points. In forward flight, however, a directivity effect may occur which makes the vibration plots look more like ellipses.

This was the case for the 2/rev IBC input, where a very irregular ellipse was formed by the sine/cosine components of the 4/rev pitching moment (Fig. 16). The irregular shape indicated nonlinear behavior, perhaps as a result of coupling with the 1/rev trim input. Since the zero-vibration origin (4 cosine = 0, 4 sine = 0) was outside the "ellipse", 2/rev amplitudes larger than two degrees would probably have been needed to reach it. However, the strong nonlinearity made it difficult to judge with any certainty.

The 2/rev IBC had the most potential to change the rotor trim. In order to maintain moment trim in the wind tunnel with 1.0 deg 2/rev IBC at 127 kts, the 1/rev cyclic input required adjustments on the order of 1.0 deg of lateral and longitudinal cyclic input, depending on the phase of the 2/rev input. This made interpretation of the effect of 1.0 deg 2/rev IBC difficult, because the changes made to the 1/rev cyclic input could significantly distort the pitch input.

However, the situation using 3/rev and 4/rev IBC to suppress vibration at 127 kts was much more promising. Unlike 2/rev IBC, the required 1/rev cyclic trim adjustments were only on the order of about 0.2 deg. Figures 17 and 18 show that 1.0 deg of 3/rev and 4/rev IBC input generated 4/rev sine-cosine ellipses which were nearly circular. This indicated a highly linear relationship between the IBC input and the 4/rev pitching moment vibration. Moreover, because the zero vibration origins and baseline points were both contained within the ellipses, suppression of the pitching moment vibration at 127 kts could most likely have been achieved using amplitudes much smaller than one degree. Given smaller input amplitudes, the 3/rev and 4/rev IBC input would have generated smaller ellipses around the baseline points. For some input phase angle, these ellipses would have gone through the zero-vibration origin. Furthermore, because Figs. 13-15 show that the in-plane forces and moments are highly coupled, it is very likely that the optimal 3/rev and 4/rev IBC inputs needed to eliminate the 4/rev pitching moment would also eliminate the rolling moment and in-plane shear forces as well. The significance of this is a reduction in the number of vibrational degrees of freedom, thereby potentially simplifying controller design. Table 5 presents the IBC amplitudes thought to be needed for vibration suppression at 43 and 127 kts.

IBC for Simultaneous BVI Noise and Vibration Control

Since 2/rev, 3/rev, and 4/rev IBC decreased the 4/rev hub moments and forces when applied separately, it was natural to question whether simultaneous BVI noise and vibration reduction might be possible using a combination of the harmonics. This idea was carefully explored at test conditions having appreciable noise and vibration. At these

Table 5.
Approximate Single-Frequency IBC Amplitudes Required for Best Vibration Control.

Harmonic	43 kts	127 kts
2/rev	3.0 deg	-------
3/rev	1.0 deg	0.25 deg
4/rev	0.75 deg	0.5 deg
5/rev	0.5 deg	*
6/rev	1.0 deg	*

*Not evaulated

test conditions, the rotor was tilted backward to simulate typical descent flight conditions producing high BVI noise levels. These trim states are identified as conditions 2 and 3 in Table 4. Both conditions simulated about a 6 deg glide slope, typical of a normal helicopter approach into the terminal area. Whereas the highest BVI noise levels were produced at the 65 kt airspeed, the highest combined noise and vibration levels were produced at 43 kts using a 4.0 deg shaft angle. Although simultaneous BVI noise and vibration control studies were conducted at both conditions, only the results from the 43 kt condition are presented herein.

Acoustic data were collected using four microphones on an advancing side traverse and three fixed microphones on the retreating side (Fig. 3). For each microphone, a band-limited sound pressure level was computed as the average energy present in the 150-1500 Hz range, corresponding to the 6th through 40th blade passage frequencies. This frequency band contained nearly all of the BVI noise energy. The reader is referred to Ref. 26 for a complete description of the acoustic data system and acoustic signal processing techniques. In order to save time, traverse sweeps under the advancing side of the rotor were performed to acquire acoustic field data only at the baseline condition (no IBC) and for the points showing the best noise and vibration reductions. Otherwise the traverse was parked at a single location to collect the acoustic data (16.41 ft ahead of the rotor shaft, Fig. 3).

Since the four microphones on the traverse and the three fixed microphones were spaced only a few feet apart, for the purposes of presentation in this paper only, the data from the microphones was averaged using the relationships

$$Adv.BVI = \left(\frac{mic1 + mic2 + mic3 + mic4}{4} \right)$$
$$Ret.BVI = \left(\frac{mic5 + mic6 + mic7}{3} \right) \quad (3)$$

where mic"x" denotes the band-limited BVI noise in db for microphone x. This formed two metrics which could be easily plotted for the comparison of the advancing and retreating side BVI noise levels. The details of the acoustic field variation with IBC is presented in Ref. 26.

Just as for the vibration cases mentioned in the preceding section, IBC was first applied one harmonic at a time at a fixed amplitude while the phase was varied. Variation of the amplitude was then done at the best phase angle(s) for combined BVI noise and vibration reduction. After the single-frequency inputs were tested, some multi-harmonic combinations were also tested.

Single-Frequency IBC Input. Figures 19 and 20 show the effect of applying 1.5 deg of 2/rev IBC at various input phase angles. In Fig. 19, the data obtained from all seven microphones has been plotted, whereas in Fig 20, only the average of the advancing and retreating side microphones has been shown. The right vertical axis indicates the change in BVI noise (in delta db) and references the advancing and retreating BVI noise metrics plotted as the dashed lines. It is seen that while the averaging process obscurred some of the BVI noise detail, the basic trends were preserved. Also shown in Fig. 20 is an index of the 4/rev hub vibration forces. This index was formed as the sum of the three indices used in the preceding section

$$Total\ Vibration = Lift + Shear + Moment \qquad (4)$$

where the lift, shear, and moment idices refer to the 4/rev vibration content of the lift force and the combined in-plane shear and moment indices of Eq. (2). This new index provided a measure of the total 4/rev vibration state. The relative contributions made by the forces and moments were not weighted in the summation. The left vertical axis indicates the percent change in the 4/rev vibration and references the solid curve.

By plotting the BVI noise metrics with the total 4/rev vibration metric, it was possible to get a complete picture of how IBC effected both the BVI noise and vibration. Figure 20 shows that simultaneous noise and vibration reduction using 1.5 deg of 2/rev input occurred using input phase angles between 0-120 deg, with the best results indicated at a phase angle of 60 deg. Amplitude variation of the 2/rev at this phase angle indicated that inputs between 1.5-2.0 deg yielded the best reductions in BVI noise and vibration (Fig. 21). A traverse sweep at this condition indicated that BVI noise reductions of up to 10 db were obtained in front of the rotor on the advancing side, with the average reductions being in the range of about 4-8 db (Fig. 22). The best reduction achieved in 4/rev vibration was on the order of about 30 percent.

Simultaneous noise and vibration reduction could not be well accomplished using 3/rev IBC. Figure 23 shows that 1.0 deg of 3/rev IBC reduced the advancing side BVI noise at all phase angles, but that the reductions in the retreating side BVI noise and 4/rev vibration ocurred at different IBC input phase angles. The phase angle of lowest vibration (135 deg) also maximized the retreating side BVI noise. An amplitude sweep at the 135 deg phase angle showed that by reducing the amplitude to 0.5 deg, a 60 percent decrease in the vibrations could be obtained along with a modest

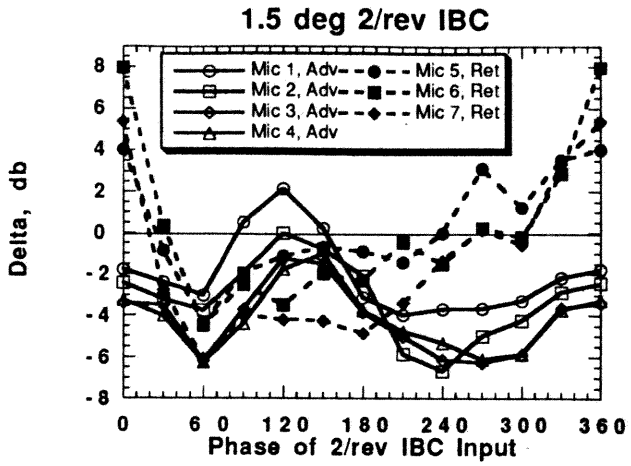

Fig. 19. Phase sweep with 2/rev IBC IBC at 1.5 deg amplitude for 43 kts, α_S= 4.0 deg, C_T/σ = 0.075.

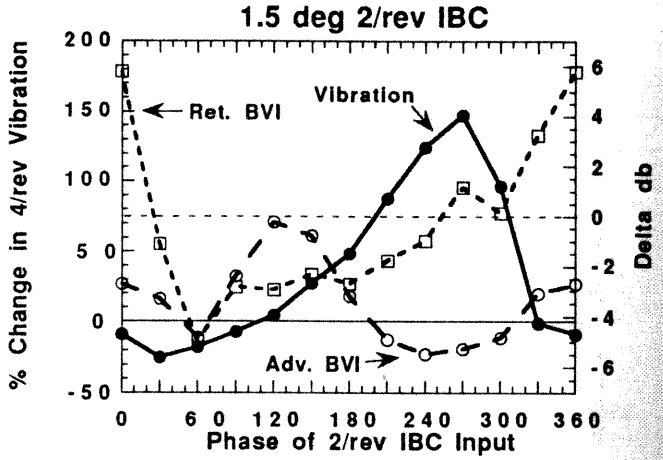

Fig. 20. Phase sweep with 2/rev IBC at 1.5 deg amplitude for 43 kts, α_S= 4.0 deg, C_T/σ = 0.075.

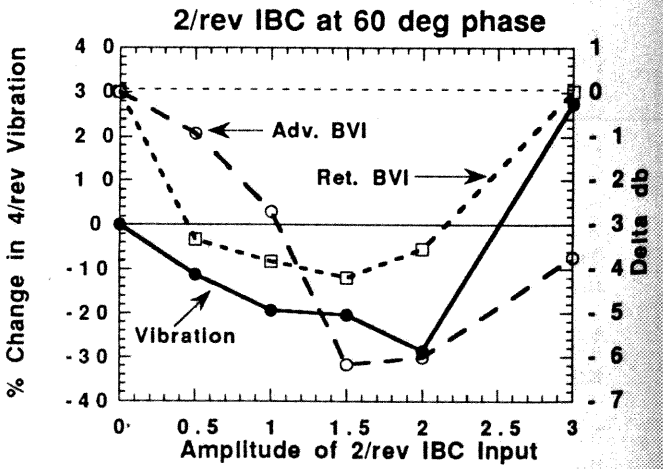

Fig. 21. Amplitude sweep with 2/rev IBC at 60 deg phase for 43 kts, α_S= 4.0 deg, C_T/σ = 0.075.

reduction in the advancing side BVI noise level (Fig. 24). However, the retreating side BVI noise level was not reduced at any amplitude. It was surprizing that the decrease in IBC input amplitude from 1.0 to 0.5 deg had such a great effect on the vibration level.

A phase sweep of 0.5 deg of 4/rev IBC showed that there was no phase which could simultaneously reduce both noise and vibration (Fig. 25). Simultaneous reduction of advancing and retreating side BVI noise was possible using 4/rev IBC input phase angles between 45 and 180 deg. Unfortunately, at these phase angles the 4/rev vibration level was increased. At 225 deg phase angle, the 4/rev input reduced the vibration by 50 percent and the retreating side BVI noise by an average of 0.5 db, but slightly increased the advancing side BVI noise by an average of 0.5 db.

Figure 26 shows that 1.0 deg of 5/rev IBC increased the 4/rev vibrations 100-200 percent. Whereas the advancing

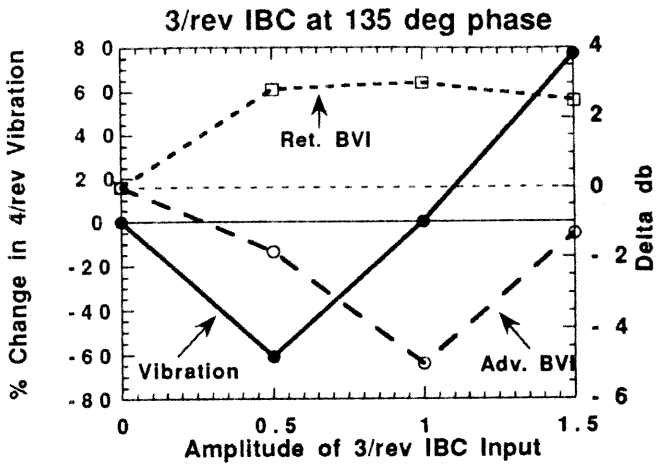

Fig. 24. Amplitude sweep with 3/rev IBC at 135 deg phase for 43 kts, α_S= 4.0 deg, C_T/σ = 0.075.

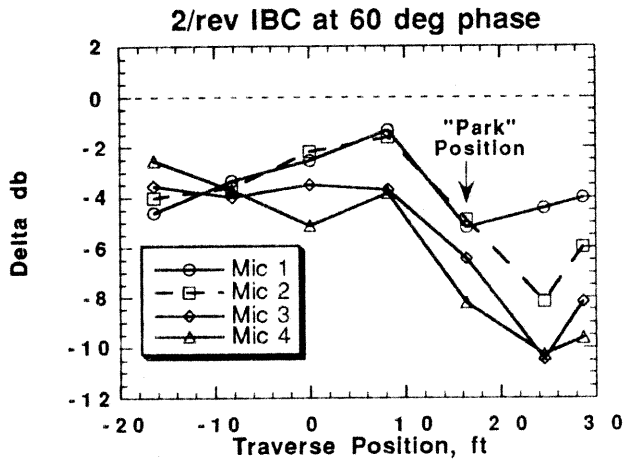

Fig. 22. Traverse sweep with 2/rev IBC at 1.5 deg amplitude and 60 deg phase for 43 kts, α_S= 4.0 deg, C_T/σ = 0.075.

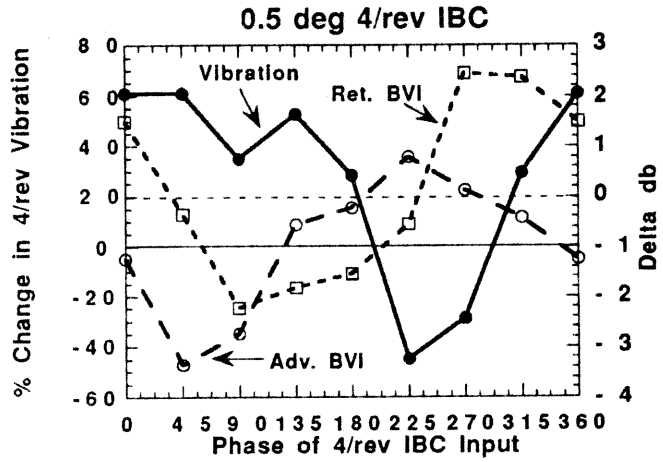

Fig. 25. Phase sweep with 4/rev IBC at 0.5 deg amplitude for 43 kts, α_S= 4.0 deg, C_T/σ = 0.075.

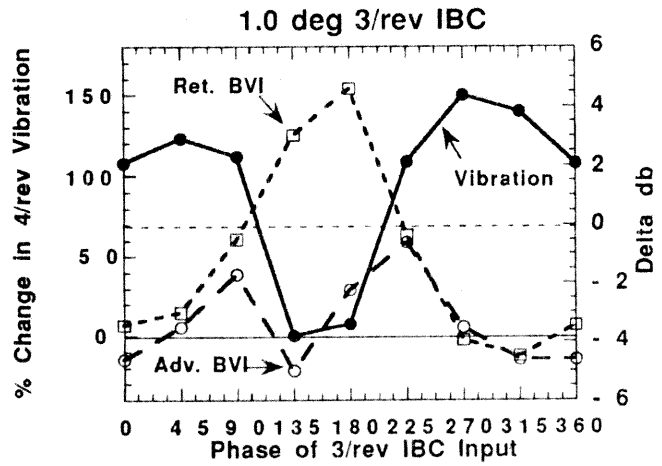

Fig. 23. Phase sweep with 3/rev IBC at 1.0 deg amplitude for 43 kts, α_S= 4.0 deg, C_T/σ = 0.075.

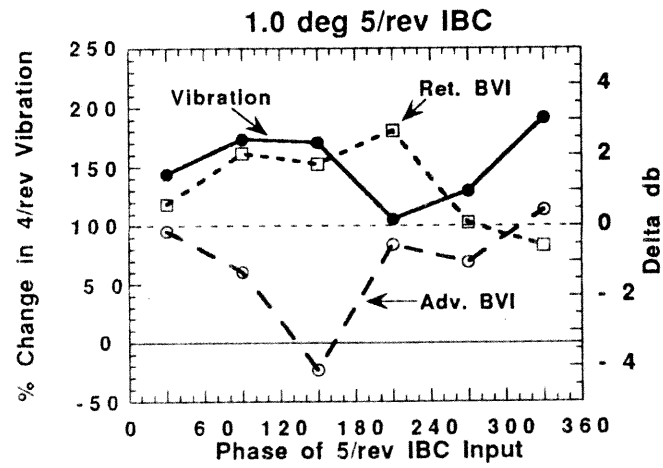

Fig. 26. Phase sweep with 5/rev IBC at 1.0 deg amplitude for 43 kts, α_S= 4.0 deg, C_T/σ = 0.075.

side BVI noise was reduced at nearly all phase angles, the retreating side BVI was usually increased. An amplitude sweep at the phase of best advancing side noise reduction (150 deg) showed that 0.5 deg and 1.5 deg 5/rev inputs did not produce further decreases in the advancing side BVI noise levels (Fig. 27). The 4/rev vibration and retreating side BVI noise levels were always higher than the baseline condition.

Limited simultaneous noise and vibration control was achieved using 6/rev IBC. Figure 28 shows that 0.5 deg of 6/rev input simultaneously reduced the vibration and BVI noise if the input phase was about 180 deg. At this input phase angle, the vibration was reduced about 20 percent and the advancing and retreating side BVI noise levels were reduced about 1 db. The best vibration reduction was obtained using a phase angle of 240 deg and the best advancing side noise reduction was obtained at 300 deg. For both of these phase angles, the retreating side BVI noise was increased. An amplitude sweep at the 240 deg and 300 deg phase angles showed that increasing the 6/rev amplitude to 1.0 deg increased the vibration and did not lower the BVI noise levels further (Figs. 29 and 30).

Multi-Frequency IBC Input. Having tested all of the single-harmonic IBC inputs, multi-harmonic input was investigated next. This was more difficult because of the large number of IBC input combinations possible.

Since the best combined noise and vibration reductions were obtained using the 2/rev input, multi-harmonic IBC combinations were investigated using 1.5 deg of 2/rev IBC at a phase angle of 60 deg as a basis. Then various other harmonics were tried in combination with 2/rev IBC.

The best simultaneous noise and vibration reductions were obtained using 2/rev and 5/rev. Figure 31 shows the results obtained by varying the phase of a 0.5 deg 5/rev input with the 2/rev input held constant at 1.5 deg amplitude and 60 deg

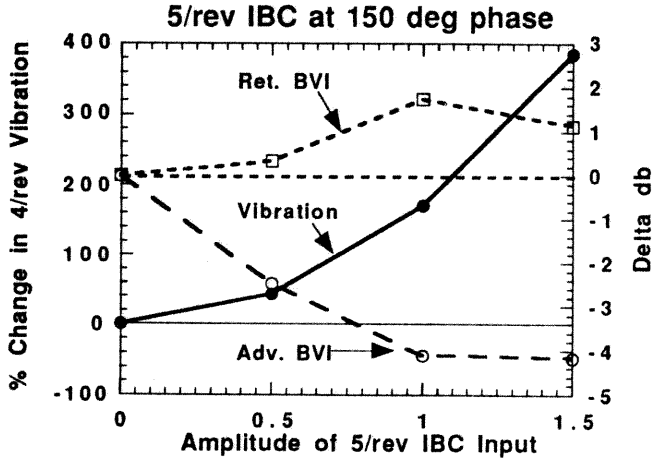

Fig. 27. Amplitude sweep with 5/rev IBC at 150 deg phase for 43 kts, α_S= 4.0 deg, C_T/σ = 0.075.

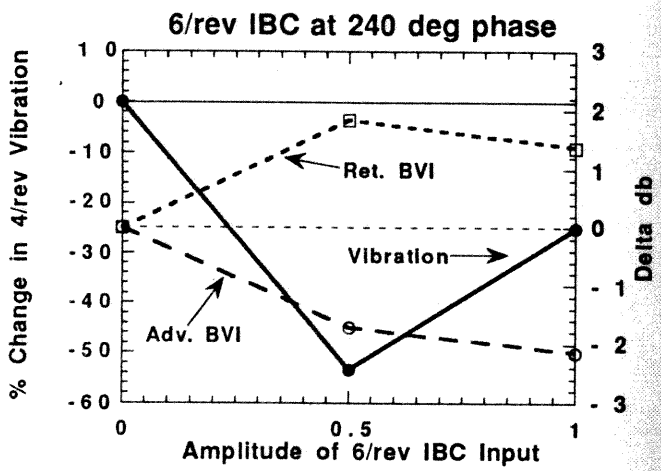

Fig. 29. Amplitude sweep with 6/rev IBC at 240 deg phase for 43 kts, α_S= 4.0 deg, C_T/σ = 0.075.

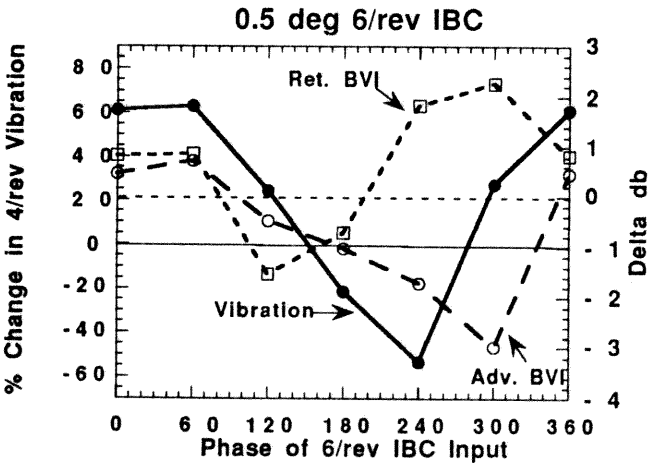

Fig. 28. Phase sweep with 6/rev IBC at 0.5 deg amplitude for 43 kts, α_S= 4.0 deg, C_T/σ = 0.075.

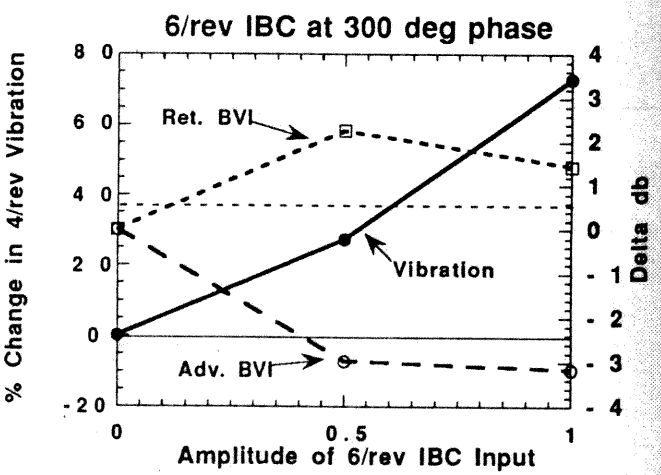

Fig. 30. Amplitude sweep with 6/rev IBC at 300 deg phase for 43 kts, α_S= 4.0 deg, C_T/σ = 0.075.

phase. At 210 deg phase, the 5/rev input simultaneously reduced the advancing side BVI noise by about 7 db, the retreating side BVI noise by 3 db, and the 4/rev vibrations by about 10 percent. Yet, compared to 2/rev alone, the retreating side BVI noise and 4/rev vibration reductions were not as great.

However, an amplitude sweep of the 5/rev input at 210 deg phase showed some remarkable simultaneous noise and vibration reductions. By reducing the amplitude of the 5/rev input to 0.25 deg, the 4/rev vibrations could be suppressed by 85 percent while reducing the advancing side BVI noise by over 10 db (Fig. 32). The retreating side BVI noise was also reduced by over 4 db at the same time. Figure 33 presents the noise reductions measured by the individual advancing side microphones during a traverse sweep of the test section at this condition. BVI noise reductions of up to 12 db were recorded at the peak advancing side BVI location.

Interestingly, Fig. 32 also shows that by raising the 5/rev IBC input to 1 deg at the 210 input phase angle, that the retreating side BVI noise could be suppressed by an average of 12 db, while still leaving the average advancing side BVI noise reduction at a respectable -6 db. Unfortunately, the 4/rev vibrations were almost doubled by the 1 deg input. This raises the question of whether another IBC input combination could achieve the 85 percent vibration reduction, while suppressing both advancing and retreating side BVI noise by 12 db.

Combinations of the other IBC harmonics were tested in the wind tunnel including 2/rev + all others, 2+4+5/rev, 2+4+6/rev, 3+4/rev, and 3+5/rev combinations. Some of these also had the ability to simultaneously suppress BVI noise and vibration, but not quite as impressively as the 2+5/rev IBC input combination.

Of all the IBC harmonics tested, this study found that only by using 2/rev IBC could the advancing side BVI noise, the retreating side BVI noise, and the vibration be appreciably reduced at the same time. The 6/rev IBC could also do this, but the gains were very modest. It also demonstrated that other IBC harmonics (such as the 5/rev) could be used to further diminish the vibration, while at the same time reducing the BVI noise by using mostly 2/rev IBC.

IBC for Reduction of Rotor Power Consumption

In principal, 2/rev IBC can be used to reduce the disk loading on the advancing and retreating sides of the rotor in order to help avoid stall and to reduce profile power losses. To maintain thrust equilibrium, the lift must be redistributed from the sides to the front and rear parts of the rotor disk. Many proponents of IBC have shown that this task can principally be fulfilled by a 2/rev IBC control input [Refs. 1-6]. Successfully implemented, this form of IBC may reduce the rotor power consumption and extend the flight envelope of the helicopter. Both a reduction of fuel weight and an

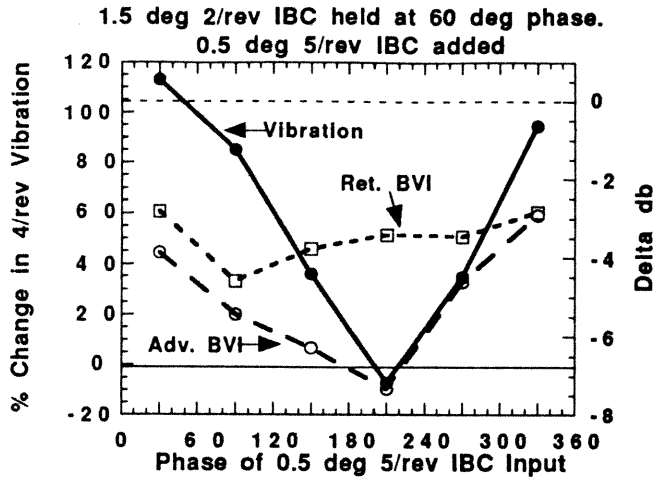

Fig. 31. Phase sweep of 0.5 deg 5/rev IBC with 2P at 1.5 deg, 60 deg phase; 43 kts, α_S= 4.0 deg, C_T/σ = 0.075.

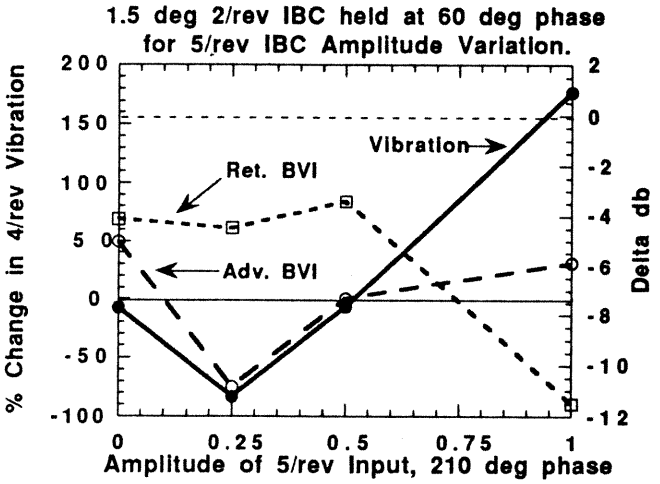

Fig. 32. Amplitude sweep of 5/rev IBC at 210 deg and 2/rev IBC at 1.5 deg, 60 deg phase; 43 kts, α_S= 4.0 deg.

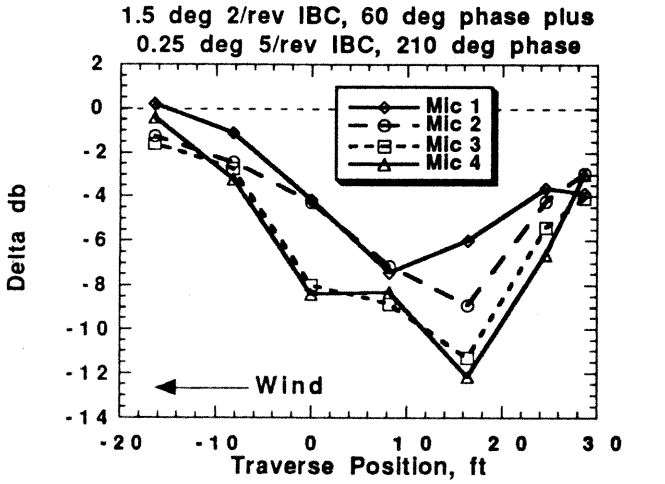

Fig. 33. Traverse sweep with 1.5 deg 2/rev IBC and 0.25 deg 5/rev IBC; 43 kts, α_S= 4.0 deg, C_T/σ = 0.075.

increase of the flight speed can lead to considerable improvements of the aircraft's productivity [Ref. 27].

In order to evaluate the power reductions due to 2/rev IBC inputs in the wind tunnel, the IBC phase was varied for several fixed IBC amplitudes and flight speeds. Conditions 4-6 of Table 4 present the rotor trim conditions. For correct evaluation of the performance benefits of IBC, considerable care was taken to keep the propulsive force, thrust, pitching moment, and rolling moment constant during the variation of the 2/rev IBC input. Keeping these quantities constant was very important because they effected the rotor blade angle of attack time history and therefore the induced and profile power contributions. In addition, three data points per IBC input were acquired in order to help reduce the effects of uncertainty in the data caused by any unsteadiness in the test conditions.

At the outset of the test, it was planned to set the rotor thrust at 1g (C_T/σ = 0.075) and the rotor shaft angle at values representative of the forward flight speeds, while at the same time maintaining a representative propulsive force. Ideally, the proper propulsive force would be that force needed to balance the drag of the aircraft,

$$Thrust \cdot Sin(-\alpha_s) = D_{EQ} \cdot q \qquad (5)$$

where D_{EQ} represents the equivalent airframe drag area (about 10-12 ft^2 for a helicopter of the BO 105 size). Although positive propulsive force was generated at all airspeeds tested, the balance needed to overcome the parasitic drag of the fuselage was only truly simulated at the μ = 0.30 (127 kt) test condition. The full propulsive force could not be developed at the higher airspeeds and shaft angles due to limitations of the collective pitch control angle. In addition, the thrust had to be slightly reduced at μ = 0.45 in order to keep the loads below the structural endurance limits. Nevertheless, some very interesting results were obtained at these airspeeds.

At 127 kts, 2/rev IBC did not show any reductions in the power consumption. Figure 34 plots the total power (measured from the rotor torque) versus the input phase angle of a 2.0 deg 2/rev IBC input at 127 kts (μ = 0.30). No performance improvement with IBC was obtained. It is very clear that the 2.0 deg input clearly caused more power consumption at most phase angles. At the worst phase angle, an increase in power consumption of 15 percent was observed.

However, at 170 kts (μ = 0.40), power reductions were obtained. Figure 35 shows that 1.0 deg of 2/rev IBC reduced power consumption up to 4 percent at input phase angles between 180-200 deg. Moreover, Fig. 36 shows that by increasing the amplitude of the IBC input, up to 7 percent power reductions were obtained at the best phase angles, with further reductions a possibility given more control authority. This reduction in power consumption equated to about a 10 percent reduction in the rotor profile power.

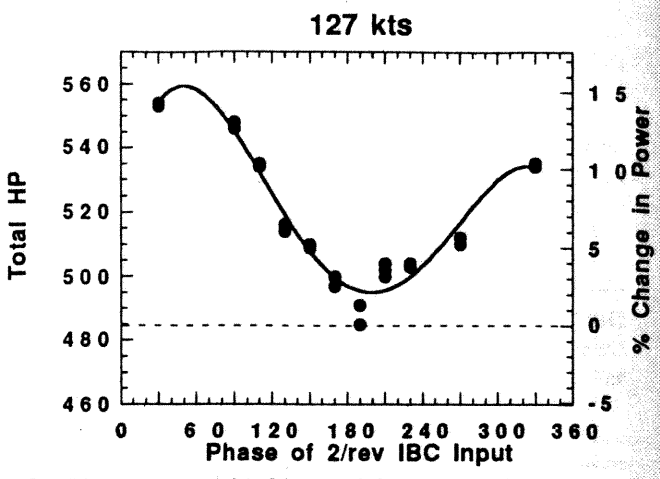

Fig. 34. Phase sweep with 2/rev at 2.0 deg amp. for 127 kts, α_S= -7.6 deg, C_T/σ = 0.075.

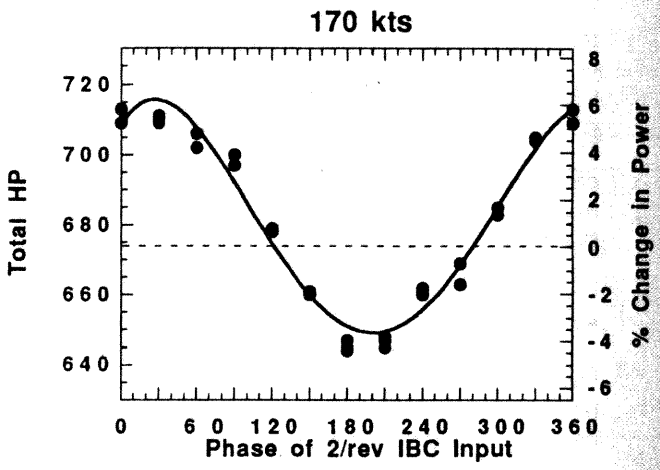

Fig. 35. Phase sweep with 2/rev at 1.0 deg amp. for 170 kts, α_S= -9.0 deg, C_T/σ = 0.075.

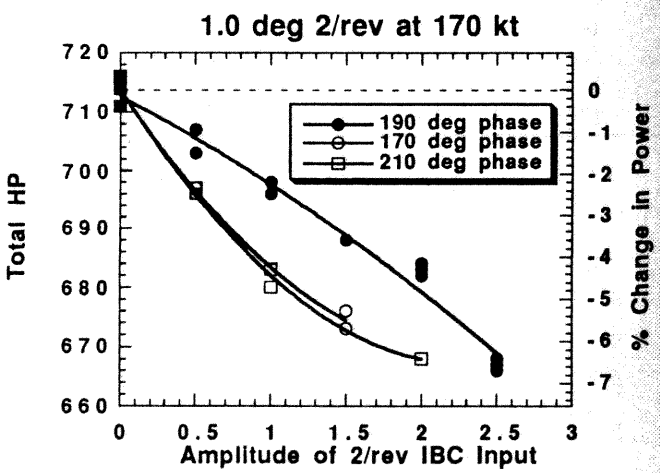

Fig. 36. 1.0 deg 2/rev IBC at 170 kt for 170, 190, & 210 deg, α_S= -9.0 deg, C_T/σ = 0.075.

At advance ratio 0.45, the IBC control authority was limited to 1.0 deg and the input phase angles between 150 deg and 210 deg in order to keep the rotor loads below the structural endurance limits. It was not possible to obtain a representative propulsive force at this airspeed because the control system limit on collective pitch angle required that the shaft angle be reduced to -8.0 deg in order to achieve a representative thrust level of (C_T/σ = 0.070). Even so, power reductions between 5 and 6 percent were observed (Fig. 37). Had it been possible to perform the testing at the correct propulsive force and nominal 1g thrust settings, larger reductions might have been possible.

The mechanism responsible for the power reductions using 2/rev IBC was obviously the creation of a more favorable blade pitch angle of attack around the rotor azimuth. This new angle of attack could have reduced power consumption by avoiding retreating side blade stall or by decreasing the profile power losses on the advancing side of the rotor. In the present wind tunnel test, blade stall was probably not a factor. Figure 38 shows that no major control loads reduction occurred at the phase angles of best power reduction (180-210 deg). Had alleviation of stall been the mechanism responsible for the power savings, a considerable reduction in the pitch link loads would have been expected. This does not mean, however, that 2/rev IBC cannot be used for stall prevention; it simply means that the rotor was probably not operating at a stalled condition in the wind tunnel, even at μ = 0.45.

The theory that the application of 2/rev IBC served to minimize the profile power losses on the advancing side of the rotor seems more plausible. Figure 39 shows a contour plot of the profile power distribution as a function of the effective angle of attack and the azimuth angle for μ = 0.40 and the radial blade location r/R = 0.9. The baseline angle of attack time history is shown together with the angle of attack time history produced by adding 1.0 deg 2/rev IBC at an input phase of 80 deg. The pitch angle time history at r/R = 0.9 was determined as the sum of the measured blade root pitch angle and the elastic blade deflection calculated from the blade tip accelerometer measurements [Ref. 23]. The profile power distribution shown in Fig. 39 was determined as a function of the effective angle of attack and the azimuth angle by using the two-dimensional airfoil drag coefficient (C_{D2D}) in the manner indicated in Ref. 28,

$$\frac{\partial P_{Profile}}{\partial r} = f\left(\alpha_{eff}, \Psi\right)$$

$$\frac{\partial P_{Profile}}{\partial r} = \frac{1}{2}\rho \cdot c \cdot C_{D2D}\left(\alpha_{eff}, \mathrm{M}(\Psi)\right) \cdot \Omega^2 R^2 \cdot (S)^{\frac{3}{2}}$$

$$S = \left(\frac{r^2}{R^2} + 2\frac{r}{R}\mu \sin\Psi + \mu^2\right) \qquad (6)$$

where, the effective Mach Number (M), angle of attach (α_{eff}), and yaw angle (Λ) were computed from

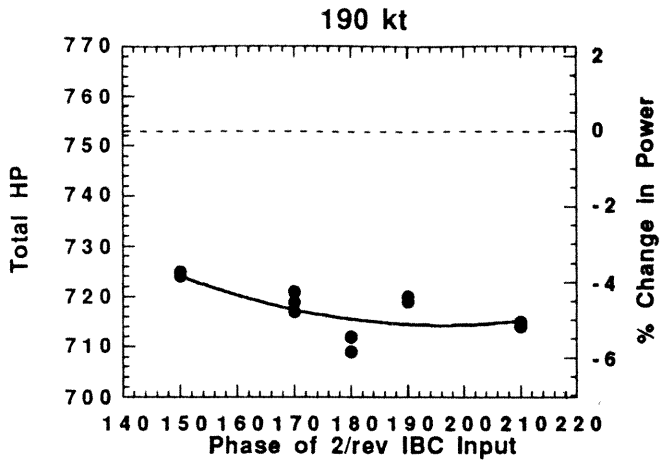

Fig. 37. Phase sweep with 2/rev at 1.0 deg amp. for 190 kts, α_S= -8.0 deg, C_T/σ = 0.070.

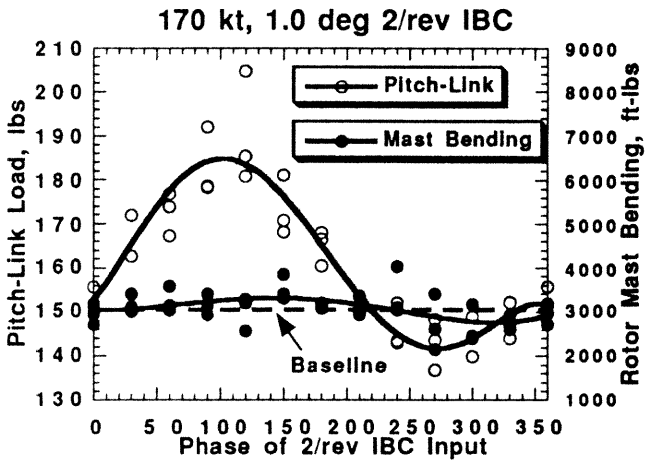

Fig. 38. Pitch link and shaft bending loads for 2/rev at 2.0 deg amp., 170 kts, α_S= -9.0 deg, C_T/σ = 0.075.

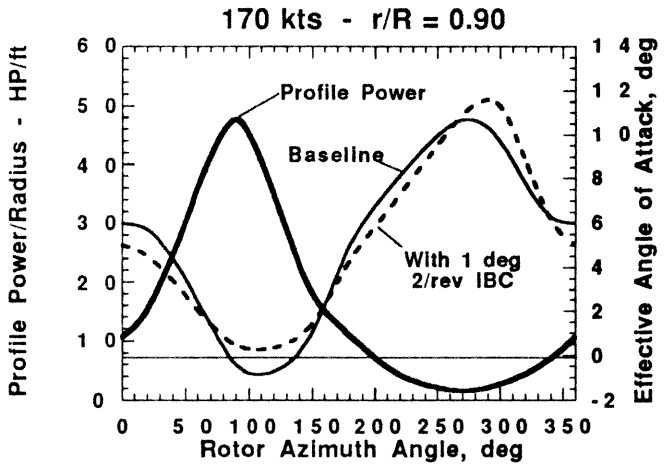

Fig. 39. Profile power and effective angle of attack, 1.0 deg 2/rev IBC at 170 kt deg, α_S= -9.0 deg, C_T/σ = 0.075.

$$M = \frac{\Omega R}{a}\left(\frac{r}{R} + \mu \cdot \sin\Psi\right) \qquad \alpha_{eff} = \alpha \cdot \cos\Lambda$$

$$\Lambda = \arccos\left(\frac{\frac{r}{R} \cdot \mu \cdot \sin\Psi}{\sqrt{S}}\right) \qquad (7)$$

Comparing the angle of attack time histories shown in Fig. 39, it is seen that the 5 percent power reduction is explained mainly by the reduced rotor blade angle of attack in the first quadrant of the rotor azimuth. The elimination of the negative angle of attack at the 90 deg azimuth position, however, actually produces an increase in the profile power. Further power savings are therefore likely given further optimization of the IBC control input in this region.

Although the reductions in power consumption were smaller than hoped for at the outset of the test, it should be recognized that these small gains are probably sufficient to off-set any extra weight or drag penalties introduced by the IBC system hardware. Moreover, since the rotor could not be operated at a stalled condition in the wind tunnel (due to limitations on the collective input), the ability of 2/rev IBC to reduce retreating blade stall was inadequately investigated. This allows the possibility for considerably higher performance improvements using 2/rev IBC at other test conditions, including those which more properly simulate the propulsive force at high speed.

Conclusions

A full-scale wind tunnel test was conducted at the NASA Ames Research Center to evaluate the potential of helicopter individual blade control (IBC) to improve rotor performance, to reduce blade vortex interaction (BVI) noise, and to alleviate helicopter vibrations. The acquired data set indicated that up to 85 percent simultaneous reductions in both BVI noise and hub vibrations could be obtained using multi-harmonic IBC input. The data also showed that performance improvements of up to 7 percent could be obtained at the higher airspeeds.

Beyond any doubt, this investigation demonstrated the importance of using 2/rev IBC to reduce helicopter BVI noise, vibration, and power consumption. Because conventional HHC systems cannot correctly apply 2/rev control to four-(or more) bladed rotors, they cannot effectively be used to simultaneously suppress both BVI noise and vibration at the same time. Nevertheless, the other harmonic inputs are very important. It was remarkable that very small amplitudes of 3/rev, 4/rev, and 5/rev IBC (0.25 deg) were seen not only to very significantly enhance the noise and vibration reductions at low-speed, but also to be useful towards reducing cruise-speed vibrations as well.

The most significant findings of this research program are summarized as follows:

1) Applied separately, 2/rev IBC was very capable of suppressing both advancing and retreating side BVI noise levels using an amplitude of 1.5 deg at the 43 kt, 6 deg glide slope descent condition. Reductions in BVI noise up to a maximum of 10 db were obtained on the advancing side of the rotor while reducing the retreating side BVI noise by an average of 4 db at the same time. Moreover, the 4/rev hub vibrations were also reduced an average of 10 percent using this input.

2) The best simultaneous noise and vibration reductions were obtained by using a combination of 1.5 deg of 2/rev IBC with 0.25 deg 5/rev IBC. This input was able to suppress the total 4/rev hub vibrations by 85 percent while simultaneously reducing the peak advancing side BVI noise up to a maximum of 12 db and the retreating side BVI noise up to 4 db at the same time. Although increasing the 5/rev input to 1.0 deg nearly doubled the 4/rev vibration, it provided an average retreating side BVI noise suppression of 12 db, while still reducing the average advancing side BVI noise by an average 6 db.

3) Simultaneous reduction of advancing side BVI noise, retreating side BVI noise, and 4/rev hub vibration was not possible using 3/rev, 4/rev, or 5/rev IBC applied alone or in combination with each other. For these harmonics, the phase angles producing the best vibration reductions are different from those required for optimal BVI noise suppression.

4) In the low-speed transition region (μ = 0.1), 2/rev, 3/rev, and 4/rev IBC, applied separately, were seen to significantly reduce the predominant 4/rev vibratory hub forces and moments. Whereas up to 80 percent simultaneous suppression of the in-plane hub forces and moments could be obtained using 2.5 deg of 2/rev IBC, up to 99 percent of the vertical shear forces could be suppressed using 1.0 deg of 3/rev IBC.

5) Vibration suppression at high-speed (μ = 0.3) may be obtained using 3/rev and 4/rev IBC input amplitudes significantly less than one deg. It is doubtful that 2/rev IBC can be used to effectively control vibration at high-speed because of its tendency to disturb the hub moment trim equilibrium.

6) With few exceptions, the vibratory hub moments and in-plane shear forces tended to be decreased (or increased) together as the IBC inputs were varied in phase and amplitude. This implies a reduction in the number of vibrational degrees of freedom from five to two (lift + 1 other) might be possible, thereby potentially simplifying controller development by reducing the measurement state vector.

7) Significant total rotor power reductions of up to 7 percent were obtained using 2/rev IBC at advance ratios higher than

μ = 0.3 (127 kts). The introduction of 2/rev IBC at μ = 0.40 to 0.45 did not significantly increase the rotor shaft bending moment or pitch-link load (IBC actuator axial load) at the phase angles of best power reduction. This allows room for further power reductions using control authorities higher than 2.5 deg.

Acknowledgments

This international research program was made possible only by the cooperation of many individuals at Ames Research Center and throughout Germany. The authors wish to thank Mr. Karl-Heinz Bock, Mr. Hans-Jurgen Goette, Mr. Thomas Schreiber, and Mr. Michael Platzer of ZF Luftfahrttechnik GmbH for their extraordinary efforts made preparing, installing, and operating the IBC system. Many thanks also go to Mr. Stephen Swanson (Sterling Software at Ames) for his help acquiring and analyzing the acoustic data. The coordination efforts under the MOU of Dr. Peter Hamel (DLR), Mr. Bernd Gmelin (DLR), Mr. Dave Key (U.S. Army), Mr. Andrew Kerr (U.S. Army), Dr. William Warmbrodt (NASA Ames), Mr. Peter Richter (ZF Luftfahrttechnik), and Dr. Dieter Braun (Eurocopter Deutschland) are also gratefully acknowledged.

References

1) Stewart, W., "Second Harmonic Control on the Helicopter Rotor", Aeronautical Research Council, Reports and Memoranda Number 2997, August, 1952.

2) Arcidiacono, P. J., "Theoretical Performance of Helicopters having Second and Higher Harmonic Feathering Control," Journal of the American Helicopter Society, Vol. 6, No. 2, April 1961.

3) Drees, J. M., and Wernicke, R. K., "An Experimental Investigation of a Second Harmonic Feathering Device on the UH-1A Helicopter," U.S. Army Transportation Research Command, TR-62-109, Fort Eustis, Virginia, June 1963.

4) McCloud, J.L., III, and Kretz, M., "Multicyclic Jet-Flap Control for Alleviation of Helicopter Blade Stresses and Fuselage Vibration", NASA SP-352, 1974.

5) Ham, N.D., "Helicopter Individual-Blade Control and its Applications", 39th Annual Forum of the American Helicopter Society, St. Louis, MO, May 1983.

6) Kretz, M., "Active Expansion of Helicopter Flight Envelope",15th European Rotorcraft Forum, Amsterdam, The Netherlands, September 1989.

7) Hammond, C.E., "Wind Tunnel Results Showing Rotor Vibratory Loads Reduction Using Higher Harmonic Blade Pitch", Journal of the American Helicopter Society, Vol. 28, No. 1, Jan. 1983.

8) Wood, E.R., Powers, R.W., Cline, J.H., and Hammond, C.E., "On Developing and Flight Testing a Higher Harmonic Control System", Journal of the American Helicopter Society, Vol. 30, No. 1, January 1985.

9) Gupta, B.P., Wood, E.R., Logan, A.H., and Cline, J.H., "Recent Higher Harmonic Control Development and OH-6A Flight Testing", 41st Annual Forum of the American Helicopter Society, Fort Worth, TX, May 1985.

10) Shaw, J., Albion, N., Hanker, E.J., and Teal, R.S., "Higher Harmonic Control: Wind Tunnel Demonstration of Fully Effective Vibratory Hub Force Suppression", 41st Annual Forum of the American Helicopter Society, Fort Worth, TX, May 1985.

11) Straub, F. and Byrns, E., "Application of Higher Harmonic Blade Feathering on the OH-6A Helicopter for Vibration Reduction", NASA CR 4031, 1986.

12) Polychroniadis, M., and Achache, M. "Higher Harmonic Control: Flight Tests of an Experimental System on SA 349 Research Gazelle", 42nd American Helicopter Society Forum, Washington, D.C., June 1986.

13) Miao, W., Kottapalli, S.B.R., and Frye, M. M., "Flight Demonstration of Higher Harmonic Control (HHC) on S-76", 42nd Annual Forum of the American Helicopter Society, Washington, D.C., June 1986.

14) Kube, R., "Evaluation of a Constant Feedback Gain for Closed Loop Higher Harmonic Control", 16th European Rotorcraft Forum, Glasgow, Scotland, September 1990.

15) Kube, R., Achache, M., Niesl, G., and Splettstoesser, W. "A Closed-loop Controller for BVI Noise Reduction by Higher Harmonic Control", 48th Annual Forum of the American Helicopter Society, Washington, D.C., June 1992.

16) Splettstoesser, W.R., Schultz, K.-J., Kube, R., Brooks, T.F., Booth Jr., E.R., Niesl, G., and Streby, O., "A Higher Harmonic Control Test in the DNW to Reduce Impulsive BVI Noise", Journal of the American Helicopter Society, Vol. 39, No. 4, October 1994.

17) Yu, Y.H., Gmelin, B., Heller, H., Philippe, J.J., Mercker, E., and Preisser, J.S., "HHC Aeroacoustics Rotor Test at the DNW - The Joint German/French/US HART Project", 12th European Rotorcraft Forum, Amsterdam, The Netherlands, October 1994.

18) Millott, T., and Friedmann, P., "Vibration Reduction in Hingeless Rotors Using an Actively Controlled Trailing Edge Flap: Implementation and Time Domain Simulation", 35th AIAA/ASME/ASCE Structures, Structural Dynamics, and Materials Conference, Hilton Head, SC, April 1994.

19) Richter, P., Eisbrecher, M.-D, and Kloppel, V., "Design and First Flight Test of Individual Blade Control Actuators", 16th European Rotorcraft Forum, Glasgow, Scotland, September 1990.

20) Teves, D., Kloppel, V., and Richter, P., "Development of Active Control Technologies in the Rotating System, Flight Testing and Theoretical Investigations", 18th European Rotorcraft Forum, Avignon, France, September 1992.

21) Jacklin, S. A., Leyland, J. L., and Blaas, A., "Full-Scale Wind Tunnel Investigation of a Helicopter Individual Blade Control System", 34th AIAA/ASME/ASCE Structures, Structural Dynamics, and Materials Conference, La Jolla, CA, April 1993.

22) Richter, P. and Blaas, A, "Full-Scale Wind Tunnel Investigation of an Individual Blade Control System for the BO-105 Hingeless Rotor", 19th European Rotorcraft Forum, Como, Italy, September 1993.

23) Jacklin, S.A., Nguyen, K.Q., Blaas, A., and Richter, P., "Full-Scale Wind Tunnel Test of a Helicopter Individual Blade Control System", 50th Annual Forum of the American Helicopter Society, Washington, D.C., May 1994.

24) Swanson, S.M., Jacklin, S.A., Blaas, A., Kube, R., Niesl, G., "Individual Blade Control Effects on Blade-Vortex Interaction Noise", 50th Annual Forum of the American Helicopter Society, Washington, D.C., May 1994.

25) Johnson, W., Helicopter Theory, Princeton University Press, New Jersey, pp. 694-698, 1980.

26) Swanson, S.M., Jacklin, S.A., Blaas, A., Niesl, G., and Kube, R., "Acoustic Results from a Full-Scale Wind Tunnel Test Evaluating Individual Blade Control", 51th Annual Forum of the American Helicopter Society, Fort Worth, TX, May 1995.

27) Vuilet, A., "The High-Speed Helicopter", 18th European Rotorcraft Forum, Avignon, France, September 1992.

28) Johnson, W., "Development of a Comprehensive Analysis for Rotorcraft I, II", *Vertica*, Vol. 5, pp. 99-129 and pp. 185-216, 1981.